

Wideband Optical Networks [WON]

Grant agreement ID: 814276

WP4 – Transceiver components design

Deliverable D4.3: InP-based coherent transmitter building blocks characterisation



This project has received funding from the European Union's Horizon 2020 research and innovation programme under the Marie Skłodowska-Curie grant agreement 814276.

Document Details

Work Package	WP4 – Transceiver components design
Deliverable number	D4.3
Deliverable Title	InP-based coherent transmitter building blocks characterisation
Lead Beneficiary:	Fraunhofer HHI
Deliverable due date:	30 April 2022
Actual delivery date:	06 June 2022
Dissemination level:	Public

Project Details

Project Acronym	WON
Project Title	Wideband Optical Networks
Call Identifier	H2020-MSCA-2018 Innovative Training Networks
Coordinated by	Aston University, UK
Start of the Project	1 January 2019
Project Duration	48 months
WON website:	https://won.astonphotonics.uk/
CORDIS Link	https://cordis.europa.eu/project/rcn/218205/en

WON Consortium and Acronyms

Consortium member	Legal Entity Short Name
Aston University	Aston
Danmarks Tekniske Universitet	DTU
VPIphotonics GmbH	VPI
Infinera Portugal	INF PT
Fraunhofer HHI	HHI
Politecnico di Torino	POLITO
Technische Universiteit Eindhoven	TUE
Universiteit Gent	UG
Keysight Technologies	Keysight
Finisar Germany GmH	Finisar
Orange SA	Orange
Technische Universitaet Berlin	TUB
Instituto Superior Tecnico, University of Lisboa	IST

Abbreviations

MZM:	Mach-Zehnder Modulator
InP:	Indium phosphide
SSC:	Spot-size converter
EO phase shifters:	Electro-optic phase shifter
MMI coupler:	Multimode interference coupler
MQW:	Multiple quantum well
TWE:	Traveling wave electrode
QCSE:	Quantum-confined Stark effect
MZI:	Mach-Zehnder Interferometer
IL:	Insertion loss
SR:	Splitting ratio
ER:	Extinction ratio
SWG:	Sub-wavelength grating
MPD:	Monitor photo diode
AR:	Anti-reflection coating
CL-TWE:	Capacitive-loaded travelling-wave-electrode

CONTENTS

LIST OF FIGURES	5
EXECUTIVE SUMMARY	6
1. Overview Transmitter, Mach-Zehnder Modulator and Components	7
2. Spot Size Converter Measurements	8
3. Splitter and Combiner	9
3.1 Three strategies for broadband MMI.....	9
3.2. MMI validation wafer layout	11
3.3 Form MMI device.....	12
4. Electro-optic phase shifter.....	13
5. Conclusions	14
6. REFERENCES	14

LIST OF FIGURES

Figure 1: Left: Principle Scheme of an InP Dual-Polarization IQ Modulator. Right: Structure of a MZM into its basic functional elements	7
Figure 2: Measured and simulated SSC loss at 1.26 – 1.37 μm and 1.47 – 1.568 μm in 20 and 40 $^{\circ}\text{C}$	8
Figure 3: Left: Schematic of geometry reconfigured MMI. Right: Optical field distribution inside MMI from top view.....	9
Figure 4: Simulated IL and SR of geometry reconfigured MMI compared with typical MMI for C band	10
Figure 5: Schematic of tunable MMI with metal pads on top.....	10
Figure 6: Simulated IL and SR of tunable MMI comparing to geometry reconfigured MMI and typical MMI for C band.....	10
Figure 7: Schematic of SWG MMI [1]	11
Figure 8: Simulated IL and SR of SWG MMI comparing with tunable MMI, geometry reconfigured MMI and typical MMI for C band.....	11
Figure 9: Left: MMI validation wafer layout. Right: One bar on the wafer. Bottom: One MMI test unit	12
Figure 10: Layer structure of geometry reconfigured MMI (left) and tunable MMI (right)	13
Figure 11: 3D illustration of tunable MMI	13
Figure 12: Measured eo-efficiency with constant and variable DC-Bias.....	14

EXECUTIVE SUMMARY

The present scientific deliverable “InP-based coherent transmitter building blocks characterisation” is part of the Work Package 4 “Transceiver components design” of the European Training Network Wideband Optical Networks (WON) funded under the Horizon 2020 Marie Skłodowska-Curie scheme Grant Agreement 814276.

The Indium Phosphide (InP) based coherent transmitter building block, which is derived from Dual-IQ Mach-Zehnder Modulator (MZM), comprises spot-size converter (SSC), splitters and combiners and electro-optic (EO) phase shifters. SSC as the interface between fiber and chip is an adiabatic taper in both horizontal and vertical direction, so that the mode of light is matched into a smaller waveguide from a larger fiber. Then, 1x2 and 2x2 multimode interference (MMI) couplers are used to split and combine lights before and after the EO phase shifter. The main structure of EO phase shifter is multiple quantum well (MQW) made in quaternary compound such as InGaAsP. RF input induces phase shift through push-pull capacitive loaded traveling wave electrode (TWE) and modulates electrical signal into the optical signal using the Quantum-Confined Stark effect (QCSE). In order to achieve high capacity optically broadband MZM, all components inside MZM must be broadband. They are supposed to operate from O to L band with stable performance and low loss. Therefore, SSC, MMI and EO phase shifter must be further improved and meet the higher requirements on operation wavelength range.

1. Overview Transmitter, Mach-Zehnder Modulator and Components

High baudrate high capacity transmitters typically incorporate Mach-Zehnder interferometer (MZI) based modulators used to modulate the light. These MZMs shall have a high electrical modulation bandwidth and a low switching voltage. Typically, the modulator is realized by dual-polarization IQ modulator, which is composed of nested MZMs. The material chosen for the WON project for these modulators is InP. InP modulators offer a strong EO effect through the use of MQW structures enabling QCSE. This strong EO-effect leads to a small half wave switching voltage $V\pi$. One crucial point about $V\pi$ is, that it is directly related to the power consumption of such transmitters.

The principle scheme of a dual IQ MZM can be found in **Error! Reference source not found.** left. The layout of chip is in a West/East configuration, with the RF coming from the East side and the optical coupling from the West side. North and South side of the chip can be used for DC fan out of all necessary contacts. Polarization rotation will be done off-chip, therefore two optical outputs are present for the TE and the TM-to-be output. The specific structure of the MZM with its functional elements is given in **Error! Reference source not found.** right.

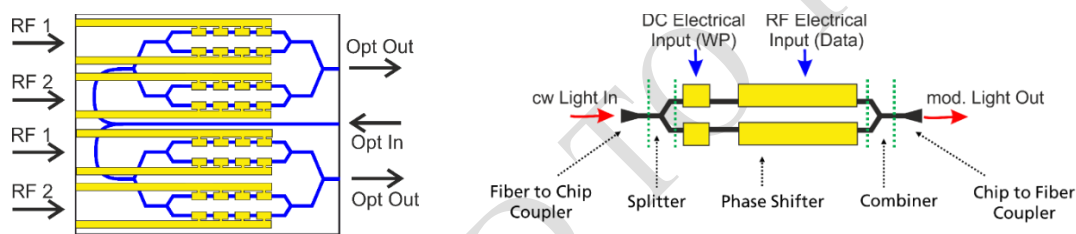


Figure 1: Left: Principle Scheme of an InP Dual-Polarization IQ Modulator. Right: Structure of a MZM into its basic functional elements

The building blocks depicted in **Error! Reference source not found.** right are listed in

	Coupler from/to Chip	Splitter/Combiner	EO-Phase Shifter
Implementation	Spot Size Converter (hor./vert. Taper)	Y-Splitter	QCSE
		1x2 MMI	Pockels
		2x2 MMI	Plasma Effect
Parameters	Loss (λ)	Splitting Ratio (λ)	Phase Shift (λ) = $V\pi(\lambda)$
		Insertion Loss (λ)	Loss (λ)
			RF Modulation Bandwidth

with possible implementation form and characteristic parameters. The Insertion Loss (IL) of an IQ Modulator is targeted not to exceed 14 dB over the entire wavelength range. Besides, $V\pi$ should not be larger than 3V and another important parameter extinction ratio (ER) is targeted to be 15 dB or better, which strongly depends on the splitting ratio (SR) of the used MMIs.

	Coupler from/to Chip	Splitter/Combiner	EO-Phase Shifter
Implementation	Spot Size Converter (hor./vert. Taper)	Y-Splitter	QCSE
		1x2 MMI	Pockels
		2x2 MMI	Plasma Effect
Parameters	Loss (λ)	Splitting Ratio (λ)	Phase Shift (λ) = $V\pi(\lambda)$
		Insertion Loss (λ)	Loss (λ)
			RF Modulation Bandwidth

2. Spot Size Converter Measurements

Since the mode size in optical fiber is much larger than that in waveguide on chip, the mode mismatch between fiber and waveguide inevitably leads to high coupling loss. Hence, the SSC is necessarily used in between, which can significantly ease the loss. SSC is typically an adiabatic taper with gradually changed width and thickness along the length. Based on guiding layer principle and adiabatic mode expansion, the mode is shaped to fit into small waveguide.

The SSC characterized and measured in this project uses InGaAsP as guiding layer material. The composition of each element in this quaternary compound must be carefully controlled, as the bandgap or luminescence wavelength should be far from the operation wavelength range to avoid absorption loss. Besides, the total loss should also be small over entire wavelength range. Figure 2 shows simulation and measurement results at 1.26 – 1.37 μm and 1.47 – 1.568 μm in 20 and 40 $^{\circ}\text{C}$. Due to the limitation on laser source and measurement setup, the measurement can only be taken on these two ranges. We can see simulated loss increases by 1 dB along wavelength due to the adiabatically changed geometry. In both ranges, the measured loss is approx. 3 dB larger than simulation results but still acceptable. The reason might be the missing focus point of the light from fiber during alignment. In 1.26 – 1.37 μm , the SSC shows a relatively stable loss around 2 ± 2 dB with the maximum loss = 4 dB at 40 $^{\circ}\text{C}$. In 1.47 – 1.568 μm , the loss is higher than before which is around 4.5 dB. SSC in high temperature has a bit higher loss than low temperature, due to the shift of the band edge of the material, but this can be neglected.

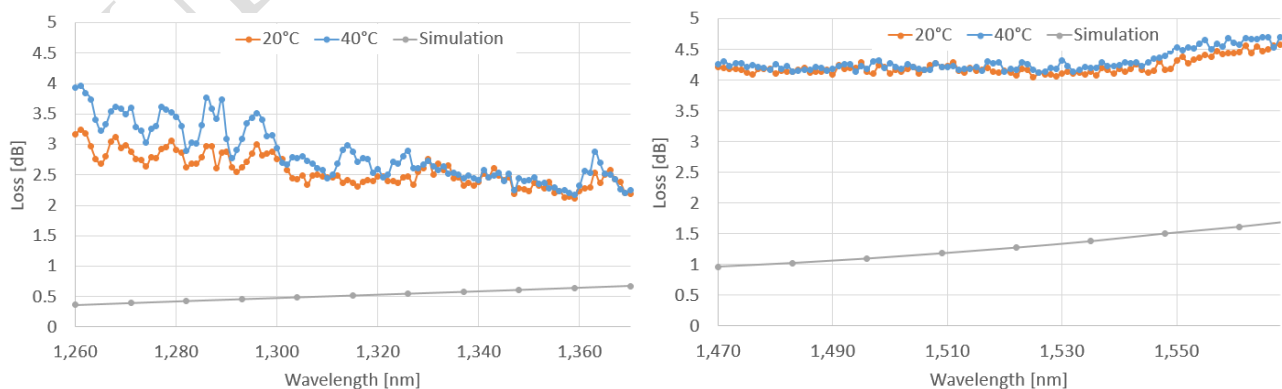


Figure 2: Measured and simulated SSC loss at 1.26 – 1.37 μm and 1.47 – 1.568 μm in 20 and 40 $^{\circ}\text{C}$

3. Splitter and Combiner

3.1 Three strategies for broadband MMI

Y-splitter and MMIs are two commonly used splitters/combiners for MZI based modulators. Since MMIs are more tolerant to fabrication variation, they are better choices than Y-splitters. Therefore, we use 1x2 MMI for light splitting and 2x2 MMI for light combining. Based on the self-imaging principle, the input image is reproduced periodically along the length of the MMI device. When the output ports are located exactly the same as the reproduction of input image, we can get uniform MMI outputs with low loss.

As MMIs are crucial components influencing the general performance of MZM, it should have stable performance over entire operation wavelength range. In our case, it's O to L band. Therefore, two important characteristic factors including insertion loss (IL) and splitting ratio (SR) must be as low as possible over this range. IL and SR characterize the loss and the uniformity at output of MMI separately. They are defined as $IL[dB] = |10 \cdot \log(P_{out1} + P_{out2})|$ and $SR[dB] = |10 \cdot \log(P_{out1}/P_{out2})|$. There are three design approaches for a constant low IL and SR. The first one is geometry reconfigured MMI. In this case, the dimension of MMI, including the length (L_{MMI}) and width (W_{MMI}) of multi-mode region and width of access waveguide (W_A) at input and output of MMI as shown in figure 3 left, are redesigned with the wavelength center at $1.45 \mu m$ instead of $1.55 \mu m$ for C band operation. As shown in simulation results in figure 4, compared to conventional MMI working on C band, a geometry reconfigured 2x2 MMI can achieve less than 1.5 dB IL over 250 nm and an SR of 1 ± 0.1 over 325 nm.

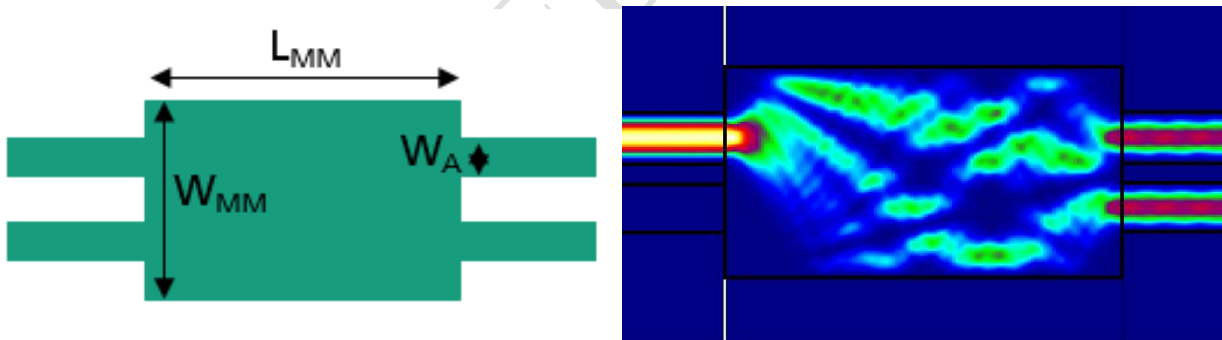


Figure 3: Left: Schematic of geometry reconfigured MMI. Right: Optical field distribution inside MMI from top view

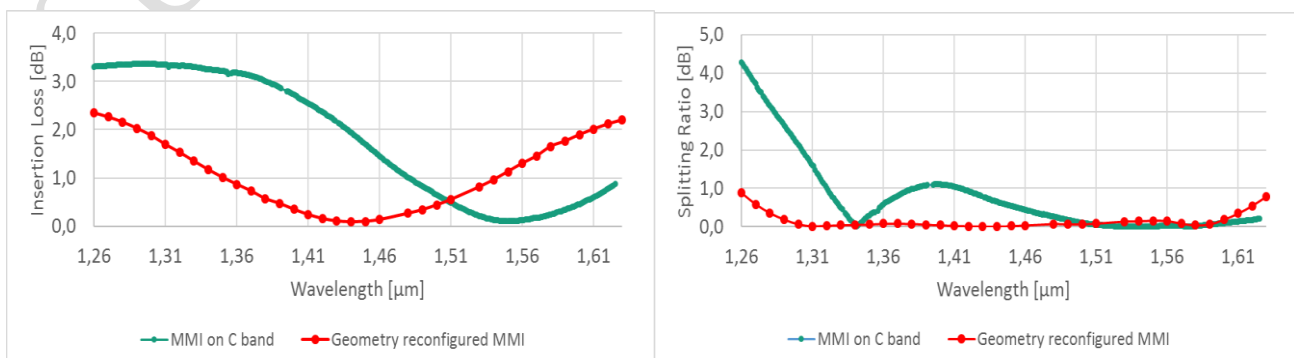


Figure 4: Simulated IL and SR of geometry reconfigured MMI compared with typical MMI for C band

The second strategy is named as tunable MMI. Similar to the working principle of optical switch, we apply a small current into the PN junction in the middle of MMI, the refractive index of light guiding layer is adjusted by the change in carrier density where current goes through. In InP based MMI used in MZM, the guiding layer mainly refers to MQW. When the light pass by these regions, the resultant phase shift of light mode by the change in refractive index is accumulated along the guiding path until the output of MMI, it then helps to balance light intensity at two output ports. As the needed phase shift changes at various wavelength points, different current input is applied. As shown in Figure 5, three metal pads are put on the surface of tunable MMI used as electric contact.

Figure 6 shows the simulation results of a tunable MMI. Same as geometry reconfigured MMI, it has almost no improvement on IL but it can improve the SR, especially at the two endpoints of operation wavelength range. For example, SR is around 1 dB smaller than geometry reconfigured MMI at 1.26 and 1.63 μm .



Figure 5: Schematic of tunable MMI with metal pads on top

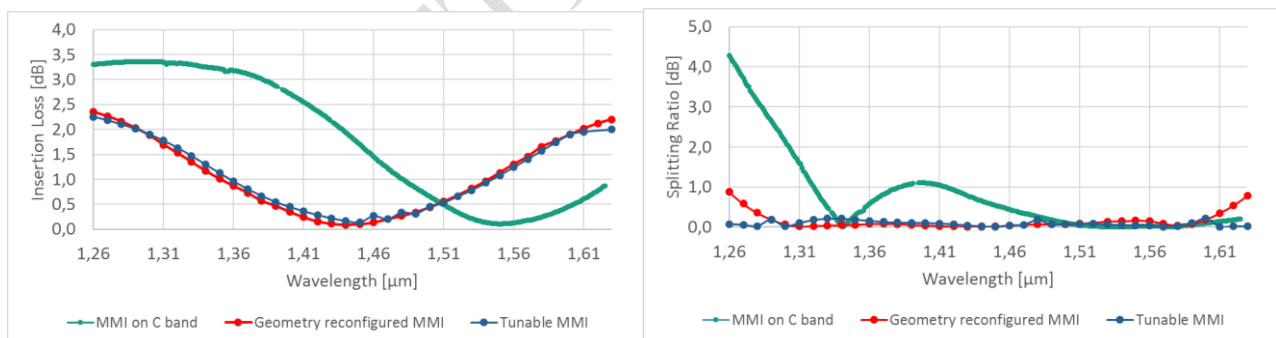


Figure 6: Simulated IL and SR of tunable MMI comparing to geometry reconfigured MMI and typical MMI for C band

The third strategy is MMI with sub-wavelength grating (SWG) structure. The MMI body is composed of thin gratings with the length of grating period equal to 0.19 μm . In contrast with single refractive index n_{core} in bulk material, SWG structure is used as artificial anisotropic material with two refractive index n_{xx} and n_{zz} in two directions. Thus, the location of reproduction of input image has less dependency on wavelength, leading to a more stable IL and SR. As shown in figure 8 left, IL has a large decrease over entire wavelength range. It is < 0.8 dB over O to L band with the maximum fluctuation = 0.2 dB. However, SR performs a slight increase compared to previous two strategies, it

is < 1 dB over most of wavelength range with the maximum fluctuation = 1dB as shown in figure 8 right.

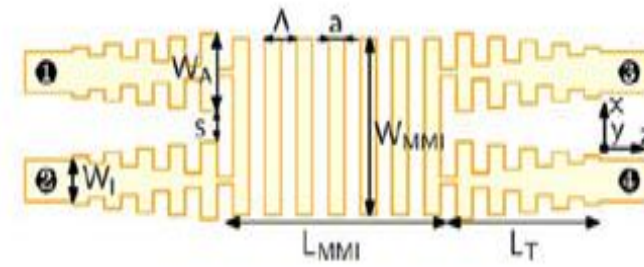


Figure 7: Schematic of SWG MMI [1]

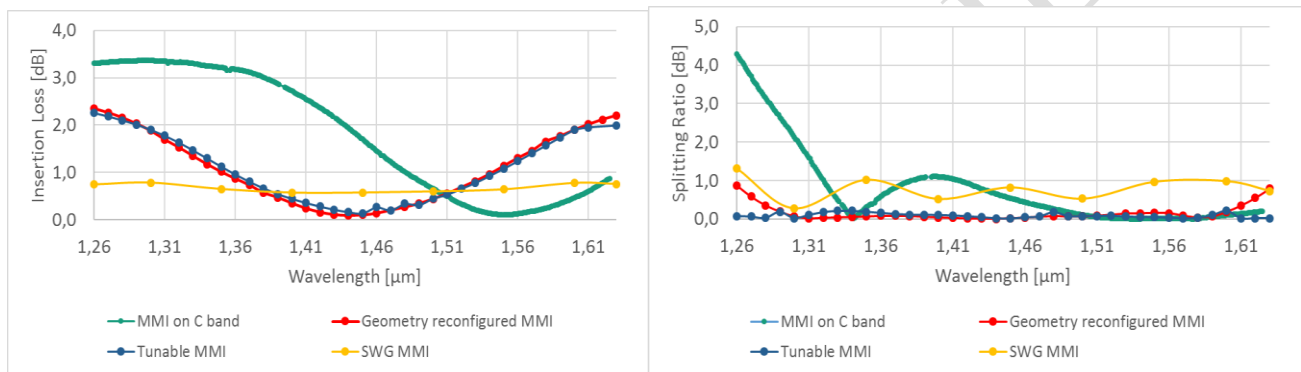


Figure 8: Simulated IL and SR of SWG MMI comparing with tunable MMI, geometry reconfigured MMI and typical MMI for C band

3.2. MMI validation wafer layout

In order to verify the simulation results of performance improved MMIs mentioned above, geometry reconfigured MMIs and tunable MMIs are fabricated. SWG MMIs are not in the schedule because of the difficulty and complexity of processing procedure. In our case, 3x3 inch wafer is used with 26 identical bars being closely placed on the wafer. Each bar has 40 MMI test units, which is composed of two MMI variants, one on chip monitor photo diode (MPD) in the middle and two SSCs at the edge of chip for light coupling from fiber. Thus, there are in total 2080 original MMIs for C band, geometry reconfigured MMIs and tunable MMIs. Each MMI variant is at least 10 times on the wafer. Hence, there are enough MMI devices for the unforeseen situations that might damage the devices during fabrication and/or testing. Besides, the large amount of MMI test devices can ensure the reliability of further measurement and analysis as well.

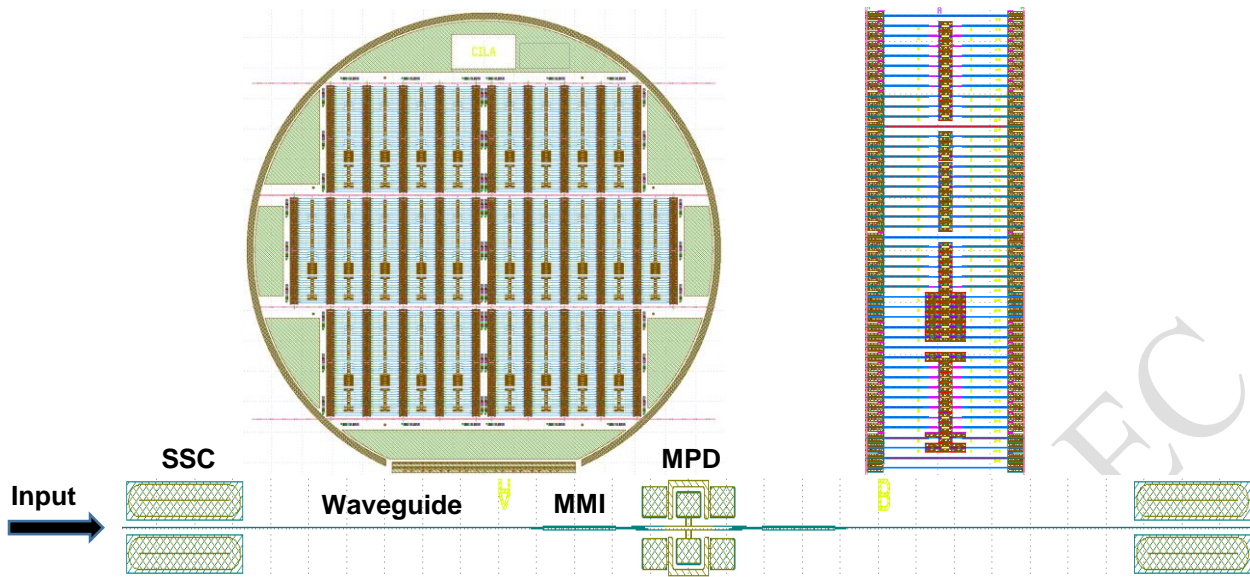


Figure 9: Left: MMI validation wafer layout. Right: One bar on the wafer. Bottom: One MMI test unit

The MMI unit is an easily used test structure comprising four main sections. As shown in figure 9 bottom, the input light is coupled from optical fiber into chip by low loss SSC, it is then guided in the waveguide to MMI test device. The core layer of waveguide must be non-absorbing over entire wavelength range to avoid absorption loss. Similar to SSC, the luminescence peak of guiding material is far away from operation wavelength. Then, the light intensity at output of MMI is converted to the photocurrent by MPD for IL and SR measurements afterwards. In contrast with SSC and waveguide, MPD uses high absorbing material to convert as much light as possible into a large enough photo current. With comparison to the photocurrent from the reference waveguide, IL and SR of MMI device can be obtained. One thing to be noted is that the second half of MMI test unit is same as the first half except the MMI device.

Other structures, for instance anti-reflection (AR) coating used on two sides of bar, can also make an impact on the final measurement. AR coating with single layer can only achieve a 10^{-3} reflection residual in the range of 10 nm around wavelength center, which can result in measurement errors. Therefore, AR coating with multiple layers is used for thorough broadband reflection.

3.3 Form MMI device

The standard MMI device processing flow based on MZM fabrication scheme mainly includes epitaxy, photolithography, wet and dry etching, metallization and electroplating. Unlike silicon platform, InP devices usually have various layers such as InP substrate, n-InP, intrinsic region containing MQW as light guiding layer and i-InP on the top. It is also the typical layer structure of geometry reconfigured MMI. It is then etched until n-doped InP layer to form MMI device body and further etched to InP substrate to electrically isolate the MMI from other devices on chip, as shown in figure 10 left. In terms of tunable MMI, p-doped InP instead of i-InP grown on most top to form inside PN junction. Besides, metallization is also implemented on tunable MMI. As shown in figure 10 right, three small metal pads are deposited on the middle region of MMI as electric contact points. A thin metal bridge is deposited

as well to connect contact points with the large contact pads outside. Electric source touches large pads directly to protect small contact points from physical damage. This processing step is electroplating. In figure 11, we can see the 3D illustration of fabricated tunable MMI device.

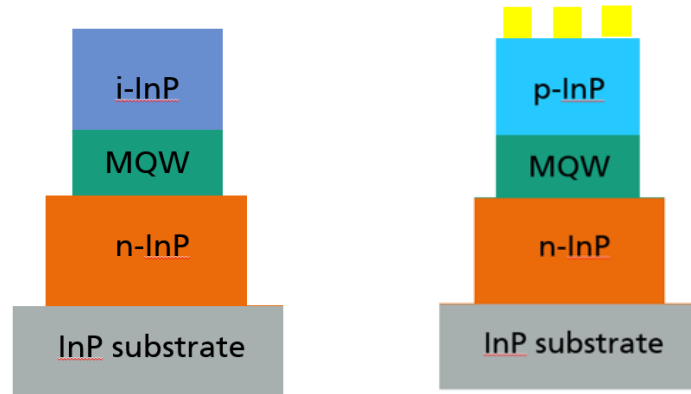


Figure 10: Layer structure of geometry reconfigured MMI (left) and tunable MMI (right)

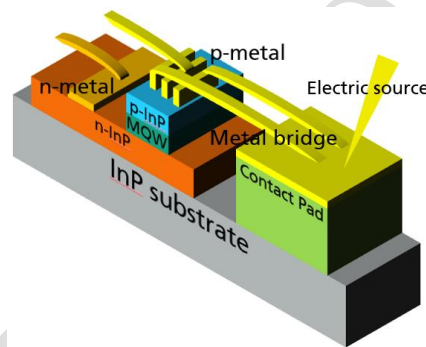


Figure 11: 3D illustration of tunable MMI

4. Electro-optic phase shifter

For the electro-optic phase-shifter we use MQWs to generate the QCSE. The QCSE is estimated to make up to 80% of the total EO phase shift efficiency, while the rest will come from the Pockels effect. The EO-effect is wavelength dependent in InP modulators with wavelength being close to the photoluminescence peak having smaller $V\pi$. Therefore $V\pi$ will always be wavelength dependent, but by carefully optimizing material composition and photoluminescence wavelength can be adjusted to achieve a \sim a factor of 2 over the desired wavelength range (see figure 12). In addition, the reverse DC bias used to pre-bias the intrinsic region can be used to compensate the variation of $V\pi$ with wavelength bringing it a further bit closer to a factor of 2 (see figure 12 as well)

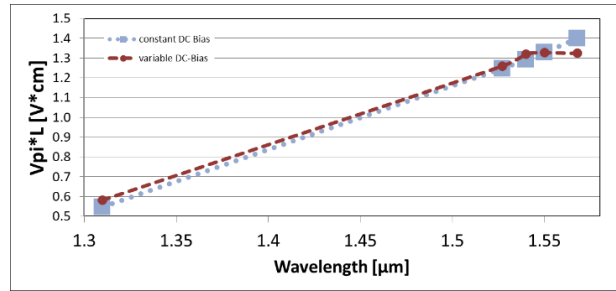


Figure 12: Measured eo-efficiency with constant and variable DC-Bias

In order to achieve the necessary RF modulation bandwidth we will implement a capacitive-loaded travelling-wave-electrode structure (CL-TWE). The CL-TWE concept is well proven, velocity matching between the optical and electrical wave is one of the parameters limiting the achievable EO bandwidth. The difference in optical group velocity between wavelength in O-Band and wavelength in L-band is not large enough to have an impact on the targeted baudrate.

5. Conclusions

In this deliverable, we presented the design concept, simulation and measurement results of SSC, MMI and EO phase shifter over O – L band (1260 – 1625 nm), which are important elements of Dual IQ MZM. For SSC, it has 2.5 – 4.5 dB loss over the entire band that is around 3 dB larger than simulation results due to limited experiment condition. So far, there are three strategies for broadband MMI with low IL and SR operating over O – L band. The tunable MMI gives the lowest SR around 0.2 dB in simulation which is 1 dB smaller than geometry reconfigured MMI at two ends of operating band, while the SWG MMI gives the most stable IL below 1dB over entire band. Only geometry reconfigured MMIs and tunable MMIs are now in processing.

6. REFERENCES

- [1] Ultra-broadband nanophotonic beamsplitter using an anisotropic sub-wavelength metamaterial; Halir, Robert, et al.; Laser & Photonics Reviews 2016